SOURCE DATA   TRANSPARENT PROCESS

LRRC25 inhibits type I IFN signaling by targeting ISG15-associated RIG-I for autophagic degradation

Yang Du[1,2,†], Tianhao Duan[1,2,†], Yanchun Feng[1,2,†], Qingxiang Liu[2], Meng Lin[2], Jun Cui[1,2,*] (iD) & Rong-Fu Wang[3,4,5,**] (iD)

Abstract

The RIG-I-like receptors (RLRs) are critical for protection against RNA virus infection, and their activities must be stringently controlled to maintain immune homeostasis. Here, we report that leucine-rich repeat containing protein 25 (LRRC25) is a key negative regulator of RLR-mediated type I interferon (IFN) signaling. Upon RNA virus infection, LRRC25 specifically binds to ISG15-associated RIG-I to promote interaction between RIG-I and the autophagic cargo receptor p62 and to mediate RIG-I degradation via selective autophagy. Depletion of either LRRC25 or ISG15 abrogates RIG-I-p62 interaction as well as the autophagic degradation of RIG-I. Collectively, our findings identify a previously unrecognized role of LRRC25 in type I IFN signaling activation by which LRRC25 acts as a secondary receptor to assist RIG-I delivery to autophagosomes for degradation in a p62-dependent manner.

Introduction

The innate immune responses, triggered by pathogen-associated molecular patterns (PAMPs), are the first line of defense against invading viruses. In virus-infected cells, viral RNAs can be detected by pattern recognition receptors (PRRs), including Toll-like receptors (TLRs), RLRs, as well as several sensors of DNA (O'Neill, 2006; Takaoka et al, 2007; Unterholzner et al, 2010; Loo & Gale, 2011; Zhang et al, 2011; Sun et al, 2013). As the major members of RLRs family, RIG-I and MDA5 (melanoma differentiation-associated gene 5) play pivotal roles in sensing cytosolic viral RNAs (Loo & Gale,

2011). Both RIG-I and MDA5 are composed of a conserved DEAD box helicase/ATPase domain, two caspase-recruiting domains (CARDs), and a C-terminal regulatory domain (CTD). Upon binding with viral RNAs via their CTD domains, RIG-I and MDA5 use their CARDs to activate downstream adaptor MAVS (also known as IPS-1, VISA, or CARDIF) (Kawai et al, 2005; Meylan et al, 2005; Seth et al, 2005; Xu et al, 2005). MAVS then triggers the signal cascades to initiate type I interferons (IFNs) production, as well as the downstream expression of multiple IFN stimulated genes (ISGs) and inflammation cytokines.

Due to its critical role in type I IFN activation, the activity of RIG-I must be tightly regulated to protect the host from uncontrolled immune response such as autoimmune disease. Several negative regulators of RIG-I have been reported to inhibit type I IFN signaling through the control of the RIG-I degradation (Arimoto et al, 2007; Chen et al, 2013; Zhao et al, 2016). RNF125 is the first reported E3 ligase, which conjugates ubiquitin to RIG-I to mediate the degradation of RIG-I through proteasome pathway (Arimoto et al, 2007). Siglec-G also promotes RIG-I degradation through enhancing K48-linked ubiquitination of RIG-I by recruiting E3 ubiquitin ligase c-Cbl (Chen et al, 2013). Recently, it has been shown that another E3 ligase CHIP associates with RIG-I and promotes RIG-I for proteasomal degradation (Zhao et al, 2016). Besides, it has been reported that RIG-I can also be conjugated by ISG15, which results in the degradation of RIG-I (Kim et al, 2008). However, the mechanisms underlying degradation of RIG-I dependent on ISG15 remain to be explored. In particular, RIG-I in general is degraded through ubiquitination-mediated proteasome pathway, and it has not been reported that RIG-I could be degraded through other degradation systems (such as lysosome and autolysosome).

Leucine-rich repeat (LRR) domain is conserved in a variety of prokaryotic and eukaryotic proteins and displays significant functions in innate immunity (Ng et al, 2011). In mammals, the functions of LRR-containing proteins, including NOD-like receptors (NLRs) and TLRs in innate immune responses, are well characterized (Inohara et al, 2005; Takeuchi & Akira, 2010). Besides NLRs

1   Zhongshan School of Medicine, Sun Yat-sen University, Guangzhou, Guangdong, China
2   Key Laboratory of Gene Engineering of the Ministry of Education, State Key Laboratory of Biocontrol, School of Life Sciences, Sun Yat-sen University, Guangzhou, Guangdong, China
3   Center for Inflammation and Epigenetics, Houston Methodist Research Institute, Houston, TX, USA
4   Department of Microbiology and Immunology, Weill Cornell Medical College, Cornell University, New York, NY, USA
5   Institute of Biosciences and Technology, College of Medicine, Texas A & M University, Houston, TX, USA
   *Corresponding author. Tel: +86 20 39943429; E-mail: cuij5@mail.sysu.edu.cn
   **Corresponding author. Tel: +1 713 441 7359; E-mail: rwang3@houstonmethodist.org
   †These authors contributed equally to this work

and TLRs, the functions of other LRR-containing proteins in innate immunity remain to be determined. In this study, we identified LRRC25 as the negative regulator of RLR-mediated type I IFN signaling. Ectopic expression of LRR-containing protein 25 (LRRC25) inhibited the phosphorylation of endogenous IRF3 and antiviral response following RLR ligand stimulation, whereas knockdown or knockout of LRRC25 had the opposite effects. Upon RNA virus infection, LRRC25 specifically interacts with ISG15-associated RIG-I to mediate RIG-I degradation via p62-dependent selective autophagy. Depletion of ISG15 abrogates RIG-I-p62 interaction as well as the autophagic degradation of RIG-I. Our findings provide new insights into the tight regulation of type I IFN signaling through its crosstalk with selective autophagy pathway and uncover a negative feedback loop to regulate RIG-I-mediated type I IFN signaling.

Results

LRRC25 inhibits RLR-mediated type I IFN signaling pathway

To identify the possible LRRC proteins that engage in type I IFN signaling pathway, we screened 22 candidate genes encoding LRRC proteins and found that LRRC25 significantly inhibited the ISRE activation induced by RIG-I CARD domains (RIG-I (N)) (Fig 1A). It has been reported that poly(I:C)-low molecular weight (LMW) is a specific ligand for RIG-I, but not for MDA5 (Kato *et al*, 2008; Takeuchi & Akira, 2010). We then analyzed the expression of LRRC25 in THP-1 cells upon challenge with vesicular stomatitis virus with enhanced GFP (VSV-eGFP), intracellular (IC) poly(I:C) (LMW), or IFN-β and found that LRRC25 protein level was up-regulated by all these treatments (Fig 1B–D). However, qPCR analysis showed that the mRNA level of *LRRC25* was not changed by these treatments (Fig EV1A). These results suggest that LRRC25 protein can be stabilized by the activation of type I IFN signaling. Furthermore, we found that type I IFN signaling stabilized LRRC25 by blocking its proteasome-dependent degradation, since the proteasome inhibitor MG132, but not the lysosome inhibitor NH_4Cl, could stabilize LRRC25 and diminish the difference of LRRC25 protein level with or without RIG-I (N)

overexpression (Figs 1E and EV1B). In addition, we found that ectopic expression of RIG-I (N) could not block the proteasome degradation of TBK1 mediated by USP38 (Lin *et al*, 2016), indicating the specific stabilization of LRRC25 mediated by RIG-I-type I IFN axis (Fig EV1C). To further test the role of LRRC25 in type I IFN signaling, we showed that LRRC25 inhibited ISRE-luc and IFN-β-luc activities after treatment with IC poly (I:C) LMW or infection with Sendai virus (SeV) (Figs 1F and G, and EV1D). However, LRRC25 had no effect on TLR3- or cGAS-mediated type I IFN activation (Fig EV1E and F), suggesting that LRRC25 specifically inhibits RLR-induced type I IFN signaling pathway. Similarly, Myc-LRRC25 significantly decreased the phosphorylation of endogenous IRF3 after treated with IC poly(I:C) LMW or infected with SeV (Fig 1H). To demonstrate a link between attenuated type I IFN response and antiviral immunity caused by LRRC25, we transfected empty vector and LRRC25 into 293T cells and subsequently infected the cells with VSV-eGFP. LRRC25 rendered the cells more susceptible to viral infection and enhanced the replication of VSV-eGFP at different time points (Fig 1I and J). Collectively, these data suggest that ectopic expression of LRRC25 markedly inhibits the type I IFN response and antiviral immunity.

LRRC25 deficiency enhances antiviral responses

To determine the physiological function of LRRC25 during RNA virus infection, we designed two LRRC25-specific small interfering RNA (siRNA) to knock down the expression of LRRC25. Both of them could efficiently knock down endogenous LRRC (Fig EV2A). To determine the effects of *LRRC25* knockdown on ISRE-luc activity, we showed that knockdown of endogenous *LRRC25* increased the ISRE-luc activity stimulated by IC poly(I:C) (Fig EV2B). Next, we tested the effect of *LRRC25* knockdown on the replication of VSV-eGFP and found that *LRRC25* knockdown substantially inhibited viral infection compared to those of cells treated with scrambled siRNA (Fig EV2C and D).

To further substantiate these findings, we used CRISPR/Cas9 system to generate *LRRC25* knockout (KO) THP-1 and 293T cells, respectively. The deletion of *LRRC25* was confirmed at the DNA and protein levels (Figs 2A and EV2E). We found that the

---

Figure 1. LRRC25 inhibits RLR-mediated type I IFN signaling pathway.

A HEK293T cells were transfected with a control plasmid or plasmids expressing 22 LRRCs along with RIG-I (N) and a reporter plasmid carrying the ISRE promoter (ISRE-Luc). 24 h after transfection, cells were analyzed for ISRE-luc activity.

B–D THP-1 cells were treated with VSV-eGFP (MOI = 0.1), intracellular (IC) poly(I:C) low molecular weight (5 μg/ml), or IFN-β (10 ng/ml) for indicated time points. Cell lysates were used for immunoblot analysis with the indicated antibodies.

E HEK293T cells were transfected with plasmids for *LRRC25*, together with an empty vector or *RIG-I (N)* for 24 h. Before harvesting, the cells were treated with DMSO or MG132 (5 μM) for 4 h. Cell lysates were used for immunoblot analysis with the indicated antibodies.

F, G HEK293T cells were transfected with plasmids for *Myc-LRRC25*, plus an *ISRE-luc* (F) or an *IFN-β-luc* (G) reporter plasmid. After 12 h, cells were treated with IC poly(I:C) LMW (5 μg/ml) or SeV (MOI = 0.1) for 24 or 14 h, respectively, and analyzed for ISRE-luc and IFN-β-luc activity.

H HEK293T cells were transfected with an empty vector or *Myc-LRRC25*. After 12 h, cells were left untreated or treated with IC poly(I:C) LMW (5 μg/ml) or SeV (MOI = 0.1) for 24 h or 14 h, respectively. Before harvesting, the cells were treated with MG132 (5 μM) for 4 h. Protein extracts were analyzed by immunoblot using the indicated antibodies.

I HEK293T cells were transfected with an empty vector (EV) or *Myc-LRRC25*. 24 h post-transfection, cells were infected with VSV-eGFP (MOI = 0.001) for the indicated time points and subjected to phase-contrast (PH) and fluorescence microscopy analyses. Scale bar, 80 μm.

J Flow cytometry analyses of 293T cells in (I). Numbers at the top-right corner indicate the percentage of cells expressing eGFP. Bar: population of GFP-positive cells.

Data information: In (B–E, H–J), data are representative of three independent experiments. In (A, F, G), data are mean values ± SEM (*n* = 3). **P < 0.01, ***P < 0.001 (Student's *t*-test).
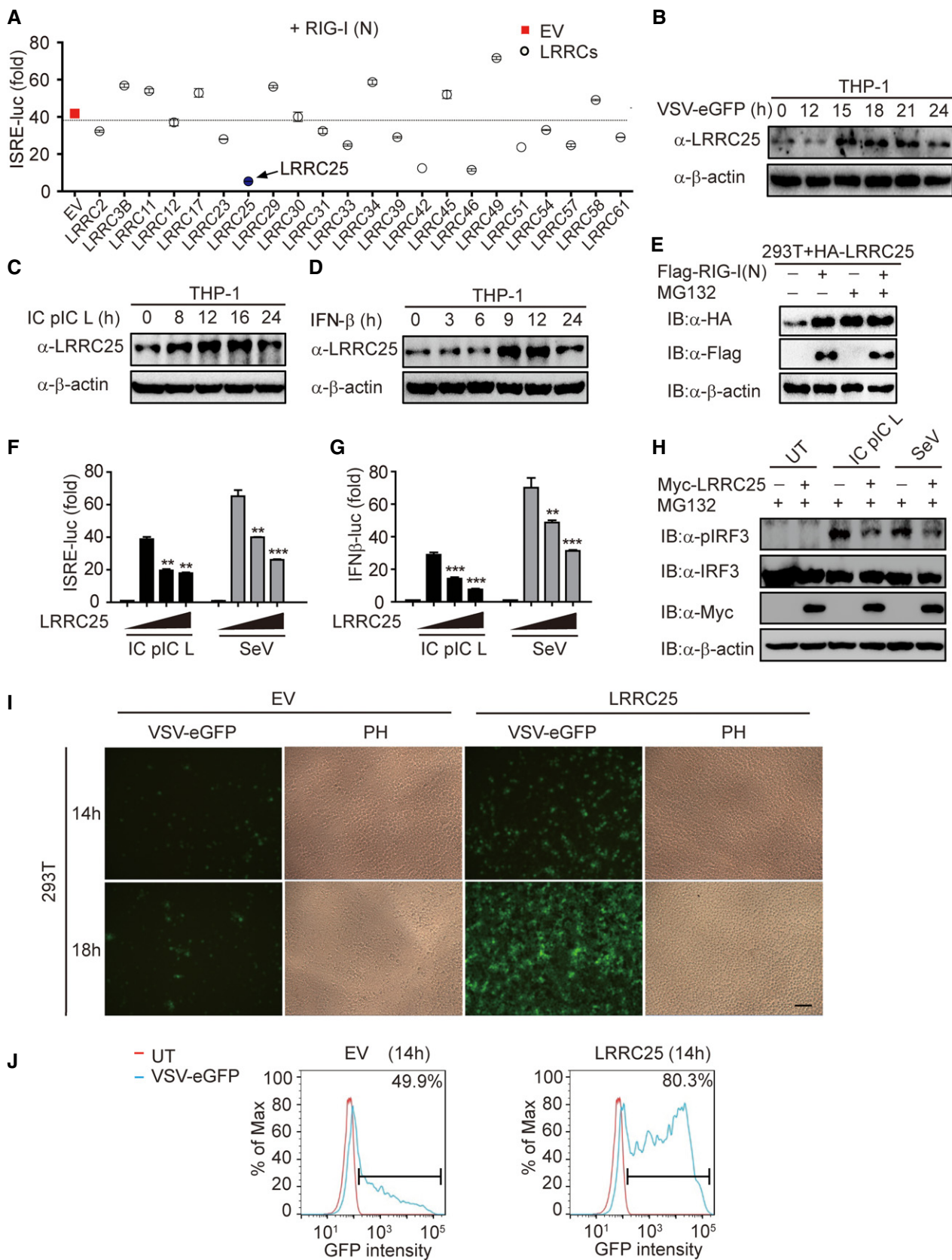Source data are available online for this figure.
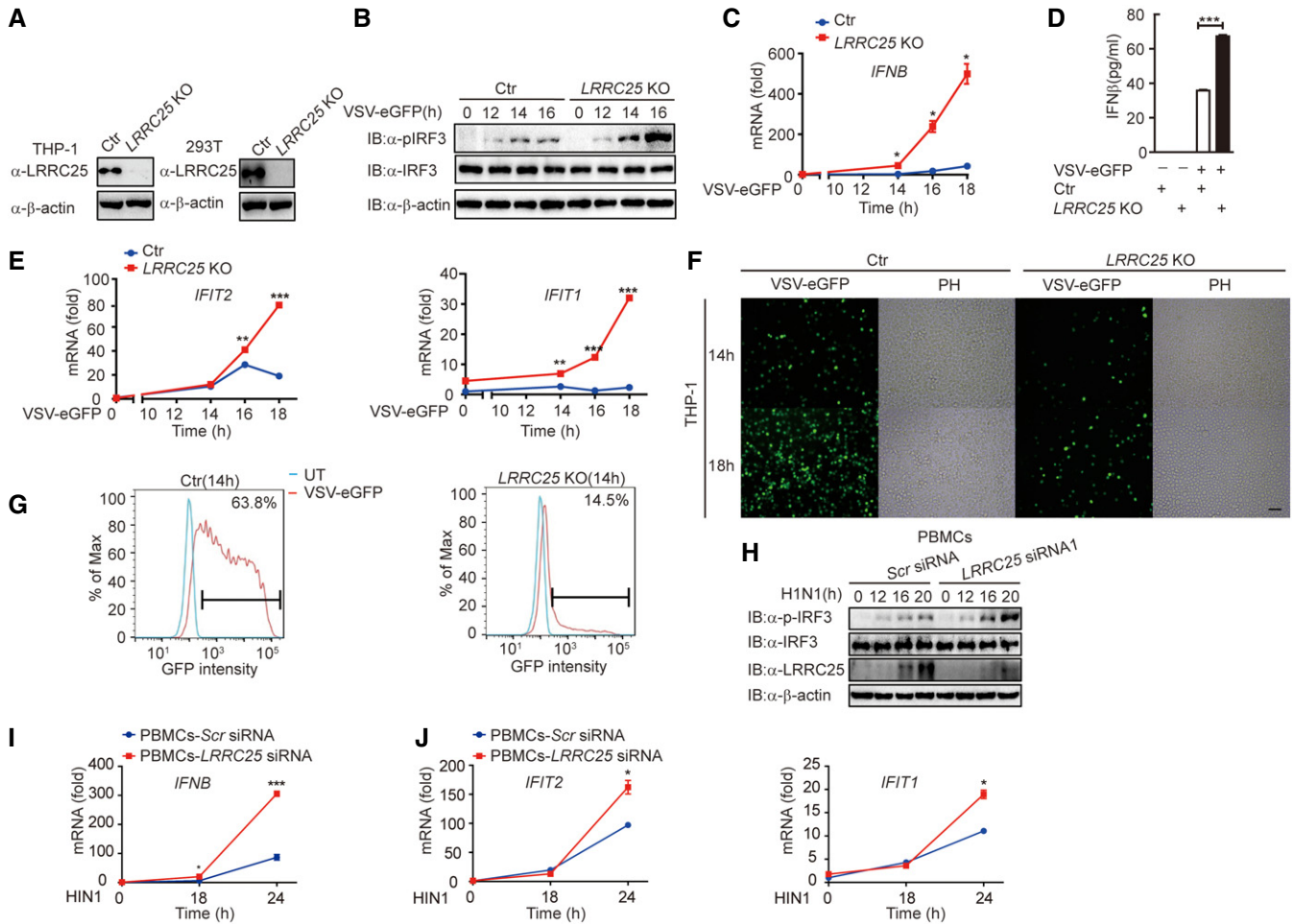
Figure 1.

Figure 2. LRRC25 deficiency enhances antiviral responses.

A   Protein extracts of control, *LRRC25* KO THP-1, and *LRRC25* KO HEK293T cells were used to perform immunoblot analysis with the indicated antibodies.

B   Control or *LRRC25* KO THP-1 cells were infected with VSV-eGFP (MOI = 0.1) for indicated time points. Cell lysates were harvested and analyzed by immunoblot.

C, D   Control or *LRRC25* KO THP-1 cells were infected with VSV-eGFP (MOI = 0.01) for indicated time points and subjected to qPCR analysis for IFN-β (C) or ELISA analysis (D).

E   Control or *LRRC25* KO THP-1 cells were infected with VSV-eGFP (MOI = 0.01) for indicated time points and subjected to qPCR analysis for *IFIT2* and *IFIT1*.

F   Control or *LRRC25* KO THP-1 cells were infected with VSV-eGFP (MOI = 0.01) for 0–18 h and subjected to phase-contrast (PH) and fluorescence microscopy analyses. Scale bar, 40 μm.

G   Flow cytometry analyses of THP-1 cells in (F). Numbers at the top-right corner indicate the percentage of cells expressing eGFP.

H   PBMCs were transfected with control or *LRRC25*-specific siRNAs for 24 h, and then, the cells were infected with influenza A/Puerto Rico/8/34 (H1N1) (PR8) (MOI = 5) for the indicated time points. Cell lysates were harvested and used to perform immunoblot analysis with the indicated antibodies.

I, J   PBMCs were transfected with control or *LRRC25*-specific siRNAs for 24 h, and then, the cells were infected with H1N1 (MOI = 5) for the indicated time points and subjected to qPCR analysis for *IFNB* (I), *IFIT2*, and *IFIT1* (J).

Data information: In (A, B, F–H), data are representative of three independent experiments. In (C–E, I, J), data are mean values ± SEM ($n = 3$). *$P < 0.05$, **$P < 0.01$, ***$P < 0.001$ (Student's *t*-test).
Source data are available online for this figure.

phosphorylation of IRF3 (p-IRF3) in *LRRC25* KO THP-1 cells was higher than that in control cells after VSV-eGFP infection (Fig 2B). We next sought to address whether the enhanced IRF3 phosphorylation by LRRC25 deficiency promotes type I IFN and ISG expressions. Using qPCR analysis, we showed that *LRRC25* KO markedly increased mRNA abundance of *IFN-β* following VSV infection (Fig 2C). Consistent with these observations, we found that VSV infection resulted in increased production of IFN-β in *LRRC25* THP-1 cells compared to control cells (Fig 2D). Consistently,

LRRC25 KO also resulted in higher expression of *IFIT1* and *IFIT2* after infection with VSV-eGFP (Fig 2E). To further investigate whether the elevated IFN response is correlated with enhanced antiviral immunity, we infected *LRRC25* KO and control THP-1 cells with VSV-eGFP. The percentage of GFP$^+$ cells increased with the extended response time, but it was markedly inhibited by LRRC25 deficiency in *LRRC25* KO THP-1 cells (Fig 2F and G). We next isolated human peripheral blood mononuclear cells (PBMCs) and knocked down endogenous LRRC25 to evaluate the physiological
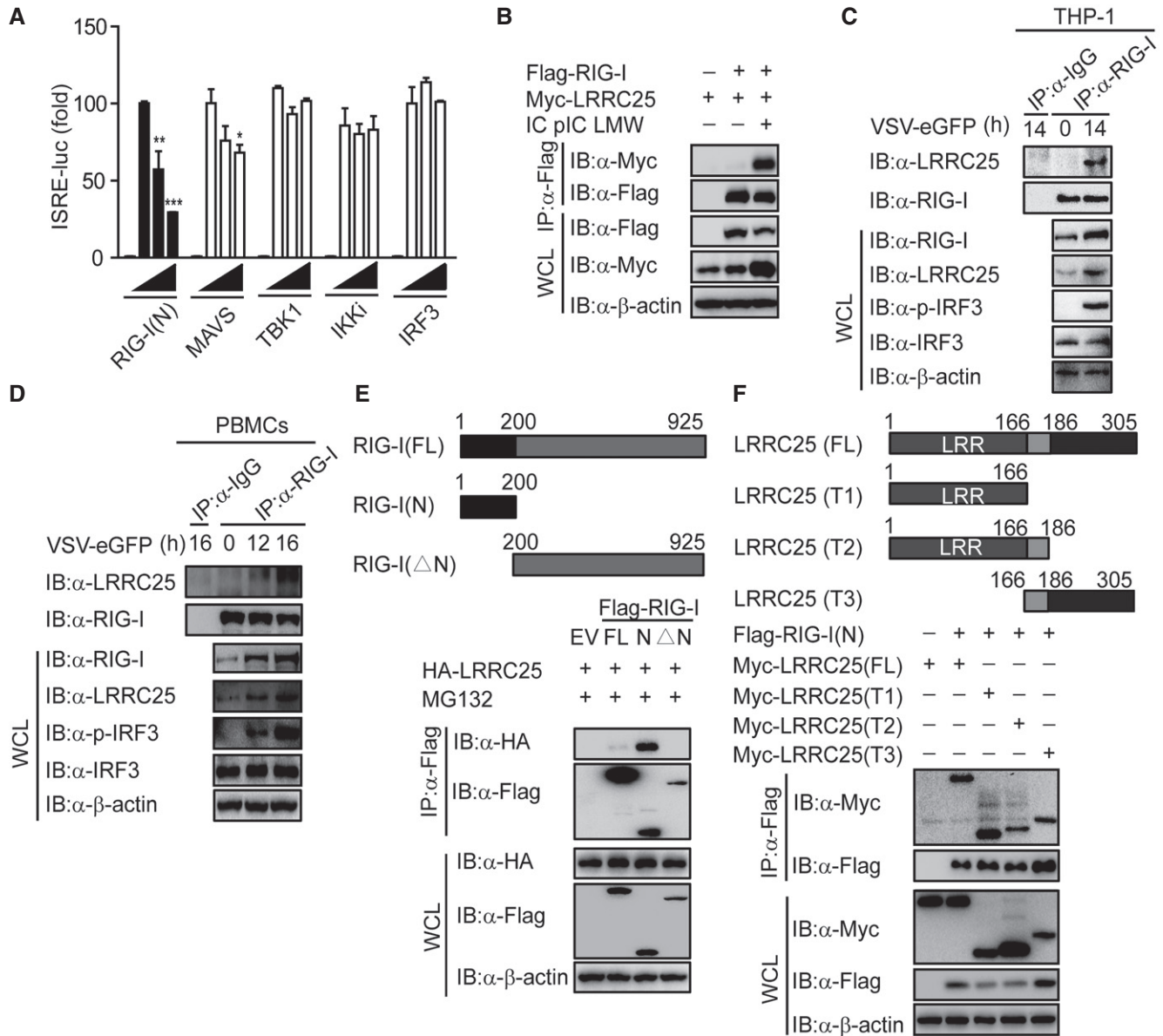
Figure 3. LRRC25 interacts with RIG-I.

A   HEK293T cells were transfected with an empty plasmid (no wedge) or increasing amounts (wedge) of plasmid for *LRRC25*, plus an *ISRE-luc* reporter and plasmids for *RIG-I (N)*, *MAVS*, *TBK1*, *IKKi* or *IRF3*. 24 h post-transfection, cell lysates were analyzed for ISRE-luc activity.

B   HEK293T cells were transfected with *Flag-RIG-I* and *Myc-LRRC25*. After 12 h, cells were left untreated or treated with IC poly(I:C) LMW (5 μg/ml) for 24 h. Cell lysates were immunoprecipitated using anti-Flag, followed by immunoblots using the indicated antibodies.

C, D   THP-1 cells (C) or PBMCs (D) were infected with VSV-eGFP (MOI = 0.1) for indicated time points, and cell lysates were immunoprecipitated using anti-RIG-I, followed by immunoblots using anti-LRRC25.

E   The structure of RIG-I and its mutants (top). HEK293T cells were transfected with deletion mutants of *RIG-I*, along with *HA-LRRC25* for 24 h. Before harvesting, the cells were treated with MG132 (5 μM) for 4 h. Cell lysates were immunoprecipitated using anti-Flag, followed by immunoblots using the indicated antibodies (bottom).

F   The structure of LRRC25 and its mutants (upper). HEK293T cells were transfected with deletion mutants of *LRRC25*, along with *Flag-RIG (N)*. 24 h post-transfection, cell lysates were harvested and immunoprecipitated using anti-Flag, followed by immunoblots using the indicated antibodies (lower).

Data information: In (B–F), data are representative of three independent experiments. In (A), data are mean values ± SEM ($n = 3$). *$P < 0.05$, **$P < 0.01$, ***$P < 0.001$ (Student's *t*-test).

importance of LRRC25 during influenza A (H1N1) infection. As expected, we found that knockdown of endogenous *LRRC25* increased the phosphorylation of endogenous IRF3 after H1N1 infection in PBMCs (Fig 2H). Furthermore, qPCR analysis showed that the deficiency of LRRC25 highly enhanced the transcription of *IFN-β, IFIT1,* and *IFIT2* upon H1N1 infection in PBMCs (Fig 2I and J).
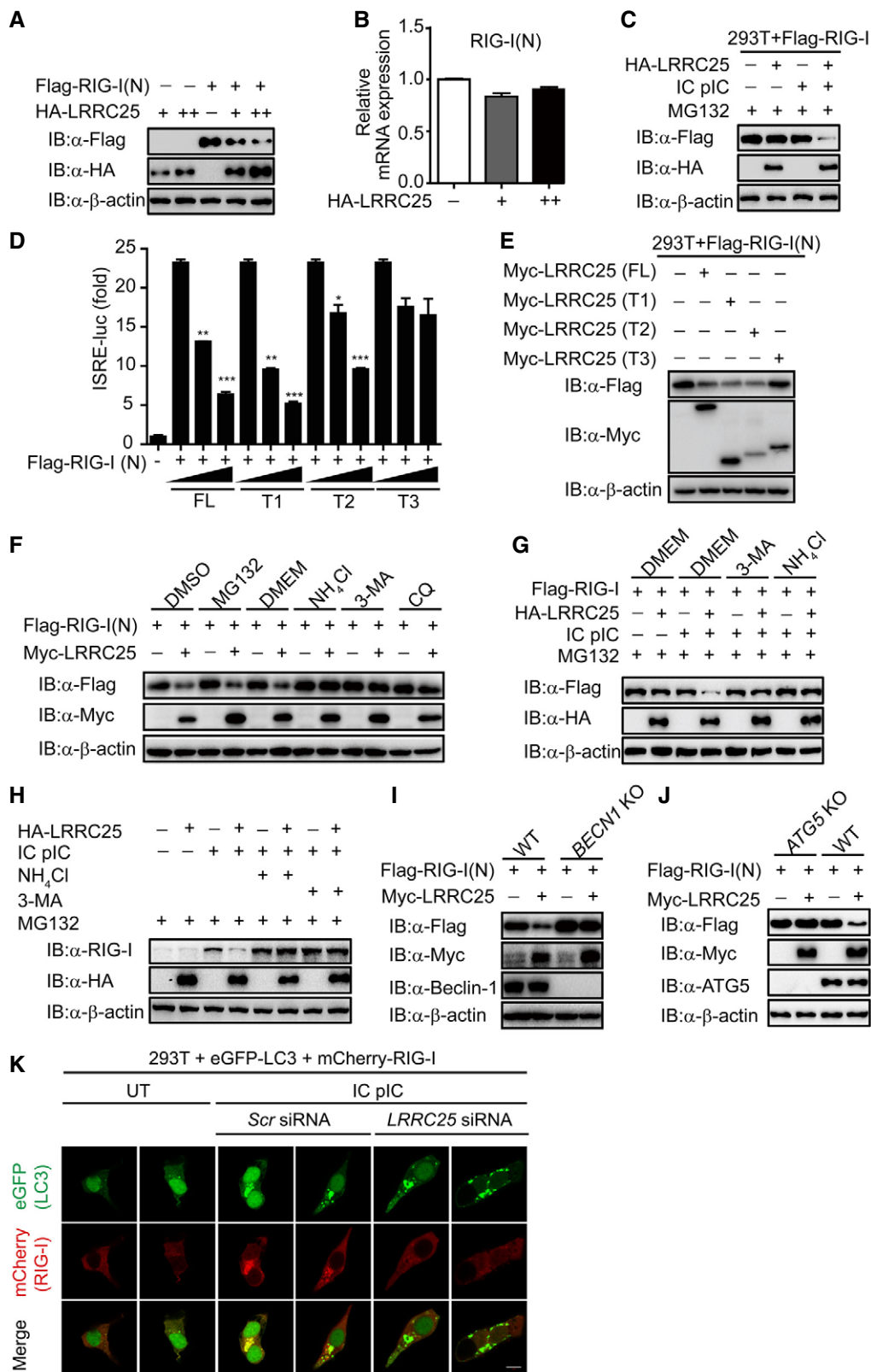
Figure 4.

Figure 4. LRRC25 targets RIG-I for autophagic degradation.

A, B HEK293T cells were transfected with *Flag-RIG-I (N)*, together with an empty vector or *HA-LRRC25* (75 and 200 ng). 24 h post-transfection, cells were harvested and used to perform immunoblot analysis with the indicated antibodies (A). Total RNA in was extracted for qPCR analysis for *RIG-I (N)* (B).

C HEK293T cells were transfected with *Flag-RIG-I* together with an empty vector or *HA-LRRC25*. After 12 h, the cells were left untreated or treated with IC poly(I:C) (5 μg/ml) for 24 h. Before harvesting, the cells were treated with MG132 (5 μM) for 4 h. Cell lysates were used for immunoblot analysis with the indicated antibodies.

D HEK293T cells were transfected with an empty vector (no wedge) or increasing amounts (wedge) of deletion mutants of *LRRC25*, along with *RIG-I (N)* and *ISRE-luc*. 24 h post-transfection, cell lysates were analyzed for ISRE-luc activity.

E HEK293T cells were transfected with *Flag-RIG-I (N)*, together with an empty vector or deletion mutants of *LRRC25*. 24 h post-transfection, cells were harvested and used to perform immunoblot analysis with the indicated antibodies.

F HEK293T cells were transfected with plasmids for *Flag-RIG-I (N)*, together with an empty plasmid or *Myc-LRRC25*. 12 h post-transfection, the cells were treated with DMSO, MG132 (5 μM), DMEM, NH$_4$Cl (10 mM), 3MA (2.5 mM), or CQ (20 μM) for 4 h, 4 h, 6 h, 6 h, 4 h, or 4 h, respectively. Cell lysates were used for immunoblot analysis with the indicated antibodies.

G HEK293T cells were transfected with *Flag-RIG-I* together with an empty vector or *HA-LRRC25*. After 12 h, the cells were left untreated or treated with IC poly(I:C) (5 μg/ml) for 24 h. Before harvesting, the cells were treated with MG132 (5 μM) for 4 h, together with DMEM, 3MA (2.5 mM), NH$_4$Cl (10 mM) for 6 h, 4 h, or 6 h, respectively. Cell lysates were used for immunoblot analysis with the indicated antibodies.

H HEK293T cells were transfected with empty vector or *HA-LRRC25*. After 12 h, the cells were left untreated or treated with IC poly(I:C) (5 μg/ml) for 24 h. Before harvesting, the cells were treated with MG132 (5 μM) for 4 h, together with DMEM, 3MA (2.5 mM), NH$_4$Cl (10 mM) for 6 h, 4 h, or 6 h respectively. Cell lysates were used for immunoblot analysis with the indicated antibodies.

I, J Wild-type (WT), *BECN* KO (I), or *ATG5* KO (J) HEK293T cells were transfected with *Flag-RIG-I (N)*, together with an empty vector or *Myc-LRRC25*. Twenty-four hours post-transfection, cells lysates were harvested and analyzed by immunoblot.

K HEK293T cells were transfected with control or *LRRC25*-specific siRNAs. 24 h post-transfection, the cells were co-transfected with mCherry-RIG-I and eGFP-LC3, followed with IC poly(I:C) (5 μg/ml) treatment for 24 h. The cells were then subjected to confocal microscopy analysis. Scale bar, 10 μm.

Data information: In (A, C, E–K), data are representative of three independent experiments. In (B, D), data are mean values ± SEM ($n = 3$). *$P < 0.05$, **$P < 0.01$, ***$P < 0.001$ (Student's *t*-test).

Taken together, these results suggest that LRRC25 deficiency strongly potentiates the type I IFN activation and antiviral immunity.

LRRC25 interacts with RIG-I

Since LRRC25 specifically inhibited RLR-mediated type I IFN signaling, we next sought to determine the molecular targets for LRRC25. We co-transfected 293T cells with *RIG-I (N)*, *MAVS*, *TBK1*, *IKKi,* and *IRF3*, together with increasing amounts of *LRRC25* plus the ISRE luciferase reporter, and found that LRRC25 markedly inhibited activation of ISRE-luc induced by RIG-I (N), but had weak or no inhibition of ISRE-luc reporter activity induced by *MAVS, TBK1, IKKi,* or *IRF3* (Figs 3A and EV3A). Furthermore, we found that LRRC25 markedly inhibited RIG-I-mediated ISRE-luc activation by IC poly(I:C) stimulation (Fig EV3B), suggesting that LRRC25 may block type I IFN signaling through active RIG-I. In addition, we observed that LRRC25 also inhibited ISRE-luc activation induced by MDA5, a RLR recognizing high molecular weight RNA fragments (Loo & Gale, 2011) (Fig EV3C).

Co-immunoprecipitation (co-IP) and immunoblot analyses further showed that LRRC25 interacted with RIG-I after IC poly(I:C) treatment (Fig 3B). To examine the physiological relevance of these findings, we infected THP-1 cells with VSV-eGFP and found that LRRC25 strongly associated with RIG-I after viral infection (Fig 3C). By contrast, LRRC25 did not associate with MAVS by IC poly(I:C) treatment (Fig EV3D). To further assess whether LRRC25 interacts with RIG-I in primary cells, we isolated PBMCs and then challenged them with VSV-eGFP and found that RIG-I strongly interacted with LRRC25 after VSV-eGFP infection in PBMCs (Fig 3D). Collectively, these data suggest that LRRC25 interacts with RIG-I after viral infection. To distinguish which domain of RIG-I was involved in the interaction with LRRC25, we constructed full-length (FL) RIG-I, truncated RIG-I (N) and RIG-I lacking CARDs (RIG-I (ΔN)), and analyzed their ability to interact with LRRC25. We found that

LRRC25 strongly interacted with RIG-I (N), but not with RIG-I (ΔN) (Fig 3E). In addition, we evaluated the interaction between LRRC25 and the CARDs of MDA5 and MAVS. We found that LRRC25 could interact with CARDs of RIG-I and MDA5, but not with CARD domain of MAVS (Fig EV3E), suggesting that the interaction between LRRC25 and CARDs of RLRs is specific. In addition, using truncated LRRC25 fragments, we found that all of the LRRC25 domains can interact with RIG-I (N) (Fig 3F). Taken together, these results suggest that LRRC25 strongly interacts with the CARD domain of RLRs.

LRRC25 targets RIG-I for autophagic degradation

We next sought to determine how LRRC25 inhibits type I IFN signaling through its interaction with RIG-I. When we transfected 293T cells with plasmids encoding RIG-I (N) and LRRC25, we found that the protein levels of RIG-I (N) were reduced with increasing LRRC25 protein expression (Fig 4A). However, LRRC25 had no effects on the mRNA level of RIG-1 (N) (Fig 4B), indicating that LRRC25 destabilized RIG-I (N) at the protein level. Consistently, we found that the concentration of RIG-I protein reduced considerably with LRRC25 expression only after IC poly(I:C) stimulation, even in the presence of MG132 (Figs EV4A and 4C). Furthermore, domain deletions of LRRC25 containing LRR could attenuate the activation of ISRE induced by RIG-I (N), as well as the abundance of RIG-I (N) (Figs 4D and E, and EV4B). In addition, we found that MDA5 protein levels decreased considerably with increased LRRC25 expression (Fig EV4C). By contrast, LRRC25 had no effects on the protein level of MAVS (Fig EV4D). Collectively, these data indicate that LRRC25 promotes the degradation of RIG-I and MDA5 after viral infection.

To determine how LRRC25 promotes the degradation of RIG-I after stimulation, we found that LRRC25-mediated degradation of RIG-I (N) was completely inhibited by NH$_4$Cl, 3-methyladenine (3MA), chloroquine (CQ), and bafilomycin A1, which are inhibitors
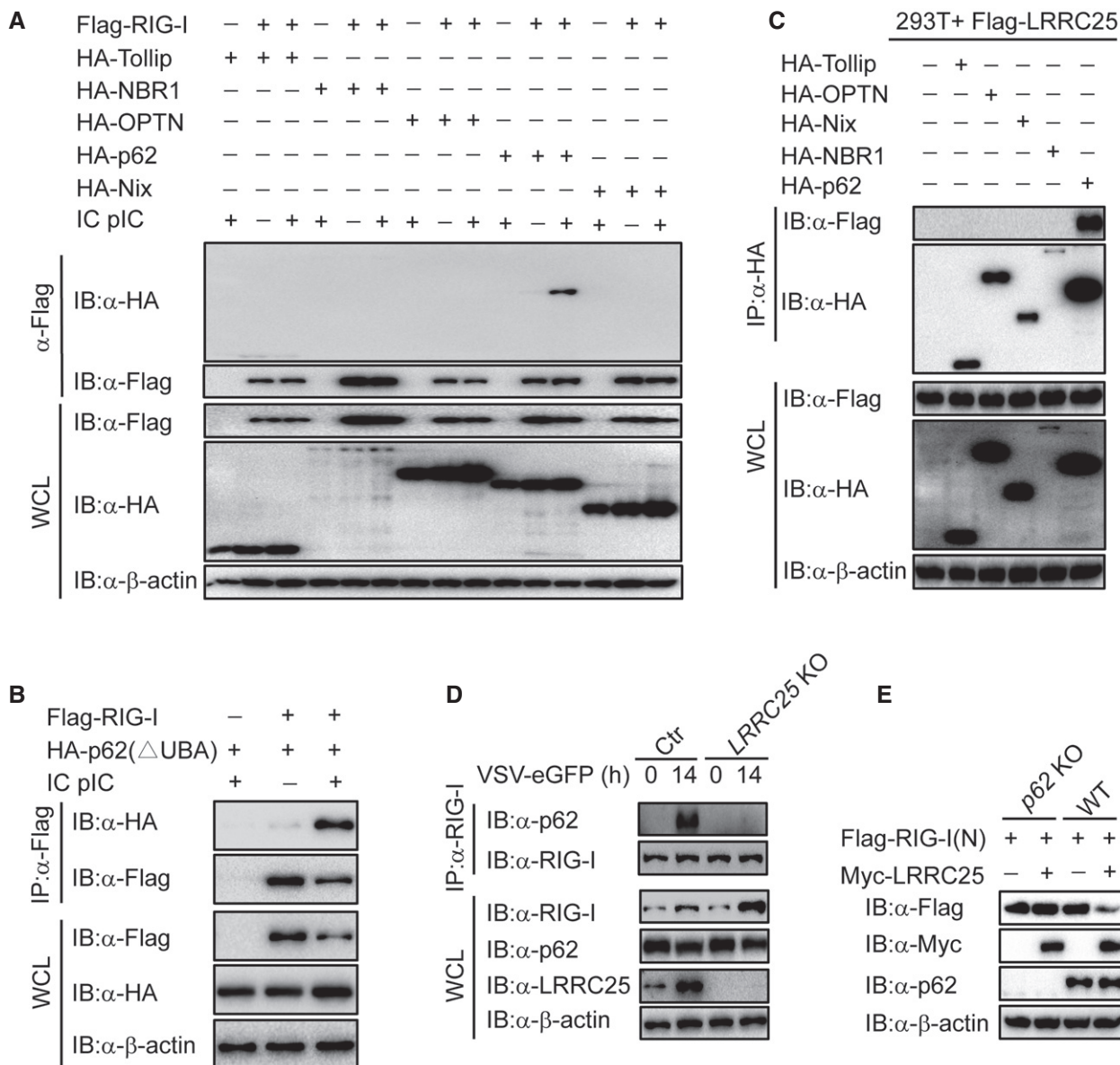
Figure 5. LRRC25 bridges RIG-I to p62 for autophagic degradation.

A   HEK293T cells were transfected with *Flag-RIG-I* together with *HA-Tollip*, *HA-NBR1*, *HA-OPTN*, *HA-p62*, or *HA-Nix*. After 12 h, the cells were left untreated or treated with IC poly(I:C) (5 μg/ml) for 24 h. Cell lysates were immunoprecipitated using anti-Flag, followed by immunoblotting using the indicated antibodies.

B   HEK293T cells were transfected with *Flag-RIG-I* and *HA-p62* (ΔUBA). After 12 h, the cells were left untreated or treated with IC poly(I:C) (5 μg/ml) for 24 h. Cell lysates were immunoprecipitated using anti-Flag, followed by immunoblots using the indicated antibodies.

C   HEK293T cells were transfected with *Flag-LRRC25*, together with expression vector of *HA-Tollip*, *HA-OPTN*, *HA-Nix*, *HA-NBR1*, or *HA-p62*. 24 h post-transfection, cells lysates were immunoprecipitated using anti-Flag, followed by immunoblot using the indicated antibodies.

D   Control and *LRRC25* KO THP-1 cells were infected with VSV-eGFP (MOI = 0.1) for 14 h. Cell lysates were immunoprecipitated using anti-RIG-I, followed by immunoblots using anti-p62.

E   WT and *p62* KO HEK293T cells were transfected with plasmids for *Flag-RIG-I (N)*, together with an empty vector or *Myc-LRRC25*. 24 h post-transfection, cell lysates were harvested and used to perform immunoblot analysis with the indicated antibodies.

Data information: In (A–E), data are representative of three independent experiments.

for lysosomal and autophagic degradation, respectively, but not MG132, which is the inhibitor for the proteasomal degradation pathway (Figs 4F and EV4E). In paralleled experiments, ectopically expressed LRRC25 could promote the degradation of FL RIG-I after IC poly(I:C) stimulation, and such degradation could be rescued by

NH_4Cl and 3MA (Fig 4G). Consistently, NH_4Cl and 3MA could block the degradation of endogenous RIG-I promoted by LRRC25 upon viral infection (Fig 4H). In addition, LRRC25 did not enhance K48-linked ubiquitination of RIG-I (N) (Fig EV4F). To further validate these results, we examined the protein level of RIG-I (N) in *BECN1*

and *ATG5* knockout 293T cells and found that blockade of the autophagy process could impair the degradation of RIG-I (N) promoted by LRRC25 (Fig 4I and J). LC3 is a well-characterized marker of the autophagy process (Kuma *et al*, 2007). We next analyzed the effect of LRRC25 deficiency on RIG-I-LC3 co-localization. As expected, we observed the puncta of RIG-I-LC3 upon IC poly(I:C) stimulation, and it was markedly inhibited by LRRC25 deficiency (Fig 4K). Taken together, these results suggest that LRRC25 targeted RIG-I for autophagic degradation.

LRRC25 bridges RIG-I to p62 for autophagic degradation

It is well documented that the removal of protein aggregates through autophagy is a highly selective process, which depends on cargo recognition by the cargo receptors (Stolz *et al*, 2014). To determine which cargo receptor was required in the degradation of RIG-I through autophagosome pathway, we examined the interactions between RIG-I and Tollip, NBR1, OPTN, p62, or Nix, respectively. We found that RIG-I specifically interacted with p62, but not with other receptors after IC poly(I:C) stimulation (Fig 5A). It is well known that ubiquitination is a targeting signal on cargoes for the recognition by the ubiquitin-associated (UBA) domain of p62. To test whether the ubiquitination of RIG-I is required for the association between RIG-I and p62, we performed co-IP analysis and showed that RIG-I could still interact with p62 ΔUBA mutant (Fig 5B), suggesting that the interaction between RIG-I and p62 does not depend on the ubiquitination of RIG-I. Furthermore, we observed that LRRC25 still reduced protein amount of RIG-I (N) (Lys 48, 99, 154, 164, 169, 172, 181, 190 arginine) (8KR), a RIG-I inactive mutant lacking all the known ubiquitination sites on RIG-I (N) in the presence of IFN-β (Fig EV4G). Together these data indicated that ubiquitination of RIG-I is not required for its degradation mediated by p62. We reasoned that LRRC25 could act as a bridge for the interaction between RIG-I and p62. As expected, the association between LRRC25 and p62, but not other receptors, was readily detected (Fig 5C). We next determined whether LRRC25 could enhance the interaction between RIG-I and p62 after VSV

stimulation. To test this possibility, we analyzed the association between RIG-I and p62 in *LRRC25* KO THP-1 cells and found that the interaction between RIG-I and p62 upon infection was abrogated in the absence of LRRC25 (Fig 5D). Furthermore, deletion of p62 in HEK293T cells completely impaired the degradation of RIG-I (N) mediated by LRRC25 (Figs 5E and EV4H). These results suggest that LRRC25 bridges RIG-I to p62 for autophagic degradation.

ISG15 serves as an essential signal for LRRC25-mediated RIG-I degradation

Our results suggest that LRRC25 mediates the degradation of RIG-I in a p62-dependent manner, once RIG-I is activated by viral infection. We next sought to determine whether the activation of type I IFN signaling or the exposure of RIG-I CARD domain serves as an essential signal for autophagic degradation of RIG-I. As MAVS is the key adaptor of RIG-I to activate downstream TBK1 and IRF3 and induces the expression of multiple ISGs, we used *MAVS* KO HEK293T cells to block the activation of type I IFN signaling and re-activated type I IFN signaling by introducing ectopic TBK1 expression to test our hypothesis (Fig 6A). As compared to wild-type 293T cells, we observed no degradation of RIG-I (N) and FL RIG-I in *MAVS* KO 293T cells, indicating that simply exposure of RIG-I CARD domain is not enough to initiate LRRC25-mediated RIG-I degradation (Fig 6B and C). Interestingly, the ability of LRRC25 to degrade RIG-I (N) was restored when we introduced ectopic TBK1 to re-activate type I IFN signaling in *MAVS* KO cells (Fig 6D). It is reported that TBK1 can also promote autophagosomal engulfment by phosphorylating p62 (Matsumoto *et al*, 2015). To exclude the possibility that TBK1 acts directly as a kinase on p62, we treated the cells with IFN-β to activate downstream ISG genes and analyzed the effect of LRRC25 on the degradation of RIG-I (N) and endogenous RIG-I. We found that LRRC25 could still attenuate the abundance of RIG-I (N) and endogenous RIG-I in the presence of IFN-β in MAVS KO cells (Fig 6E and F), which further validates that the activation of type I IFN signaling is an essential signal for autophagic degradation of RIG-I. It has been reported that ISG15, an IFN-inducible protein,

Figure 6. ISG15 serves as an essential signal for LRRC25-mediated RIG-I degradation.

A   The experimental strategy to investigate whether LRRC25 needs downstream signal to degrade RIG-I.

B   Wild-type (WT) and *MAVS* KO HEK293T cells were transfected with plasmids for *Flag-RIG-I (N)*, together with an empty vector or *HA-LRRC25* for 24 h. Before harvesting, the cells were treated with MG132 (5 μM) for 4 h. Cell lysates were harvested and used to perform immunoblot analysis with the indicated antibodies.

C   WT and *MAVS* KO HEK293T cells were transfected with *Flag-RIG-I*, together with an empty vector or *HA-LRRC25*. After 12 h, the cells were left untreated or treated with IC poly(I:C) (5 μg/ml) for 24 h. Before harvesting, the cells were treated with MG132 (5 μM) for 4 h. Cell lysates were used for immunoblot analysis with the indicated antibodies.

D   *MAVS* KO HEK293T cells were transfected with *Flag-RIG-I (N)* together with an empty vector, *Flag-TBK1*, or *HA-LRRC25* for 24 h. Before harvesting, the cells were treated with MG132 (5 μM) for 4 h. Cell lysates were harvested and used to perform immunoblot analysis with the indicated antibodies.

E   *MAVS* KO HEK293T cells were transfected with *Flag-RIG-I (N)* together with an empty vector or *Myc-LRRC25* for 24 h. Before harvesting, the cells were treated with IFN-β (10 ng/ml) and MG132 (5 μM) for 8 and 4 h, respectively. Cell lysates were harvested and used to perform immunoblot analysis with the indicated antibodies.

F   *MAVS* KO HEK293T cells were transfected with an empty vector or *Myc-LRRC25*. After 12 h, the cells were left untreated or treated with IC poly(I:C) (5 μg/ml) for 24 h. Before harvesting, the cells were treated with IFN-β (10 ng/ml) and MG132 (5 μM) for 16 and 4 h, respectively. Cell lysates were used for immunoblot analysis with the indicated antibodies.

G   *MAVS* KO HEK293T cells were transfected with *Flag-RIG-I (N)*, together with an empty vector, *ISG15,* or *HA-LRRC25*. 24 h post-transfection, cell lysates were harvested and used to perform immunoblot analysis with the indicated antibodies.

H   WT and *ISG15* KO COS7 cells were transfected with *Flag-RIG-I (N)*, together with an empty vector or *HA-LRRC25*. 24 h post-transfection, cell lysates were harvested and analyzed by immunoblot.

I   WT and *ISG15* KO COS7 cells were transfected with an empty vector or *Myc-LRRC25*. After 12 h, the cells were left untreated or treated with IC poly(I:C) (5 μg/ml) for 24 h. Before harvesting, the cells were treated with MG132 (5 μM) for 4 h. Cell lysates were used for immunoblot analysis with the indicated antibodies.

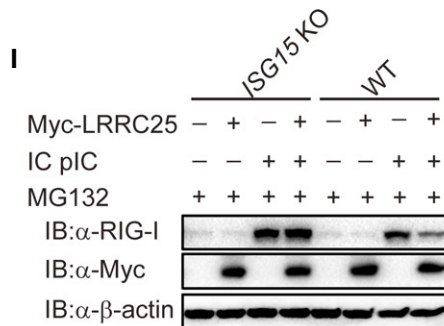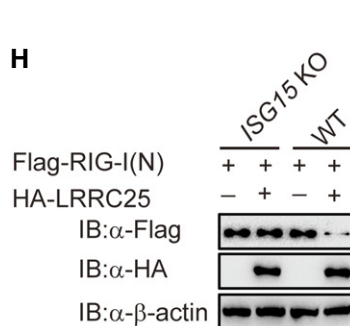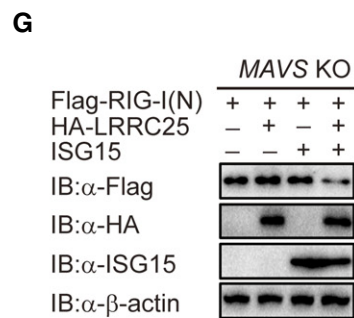Data information: In (B–I), data are representative of three independent experiments.
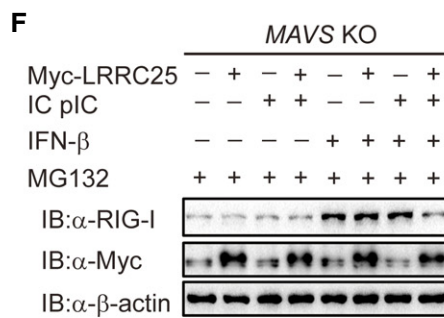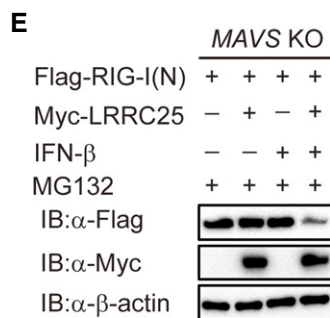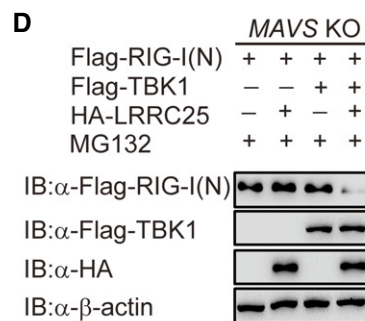
Figure 6.

Figure 7. The interaction between RIG-I and LRRC25 is dependent on ISG15.

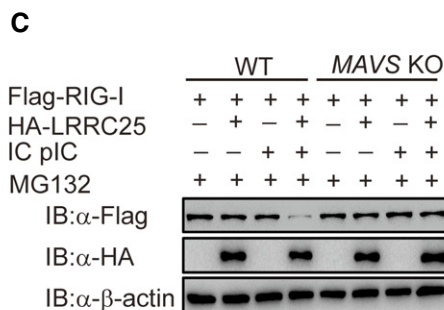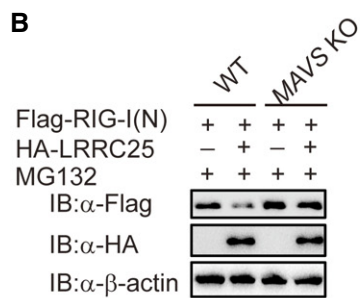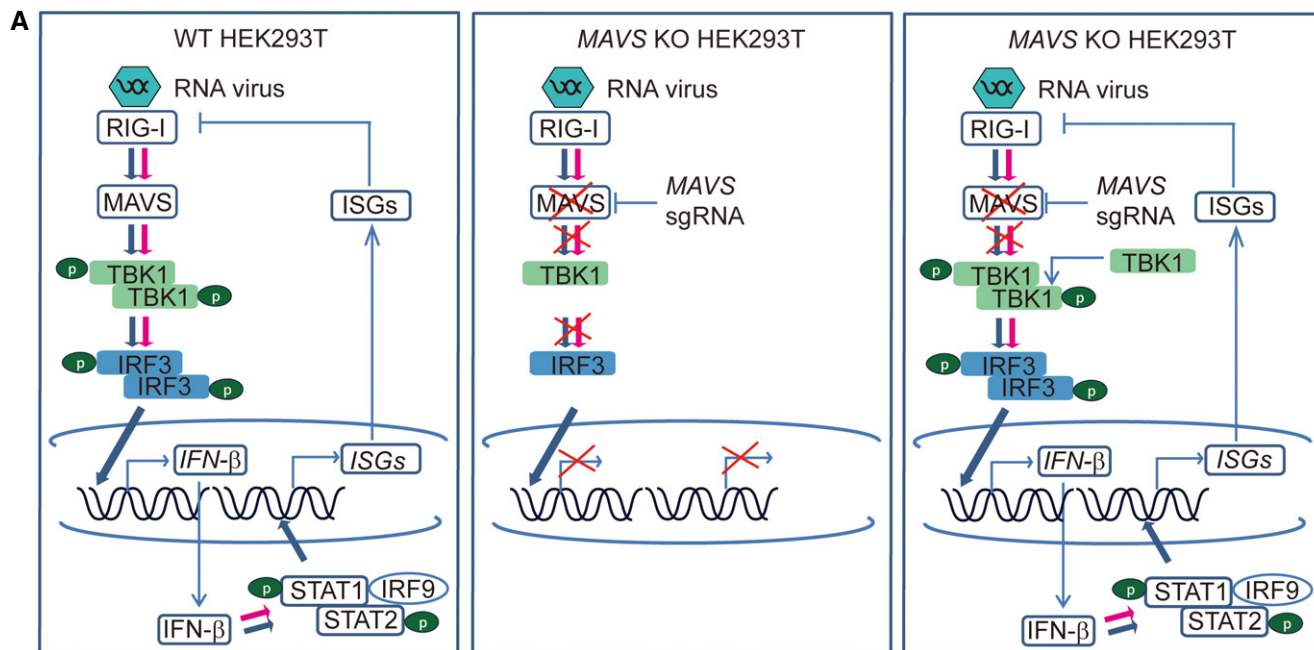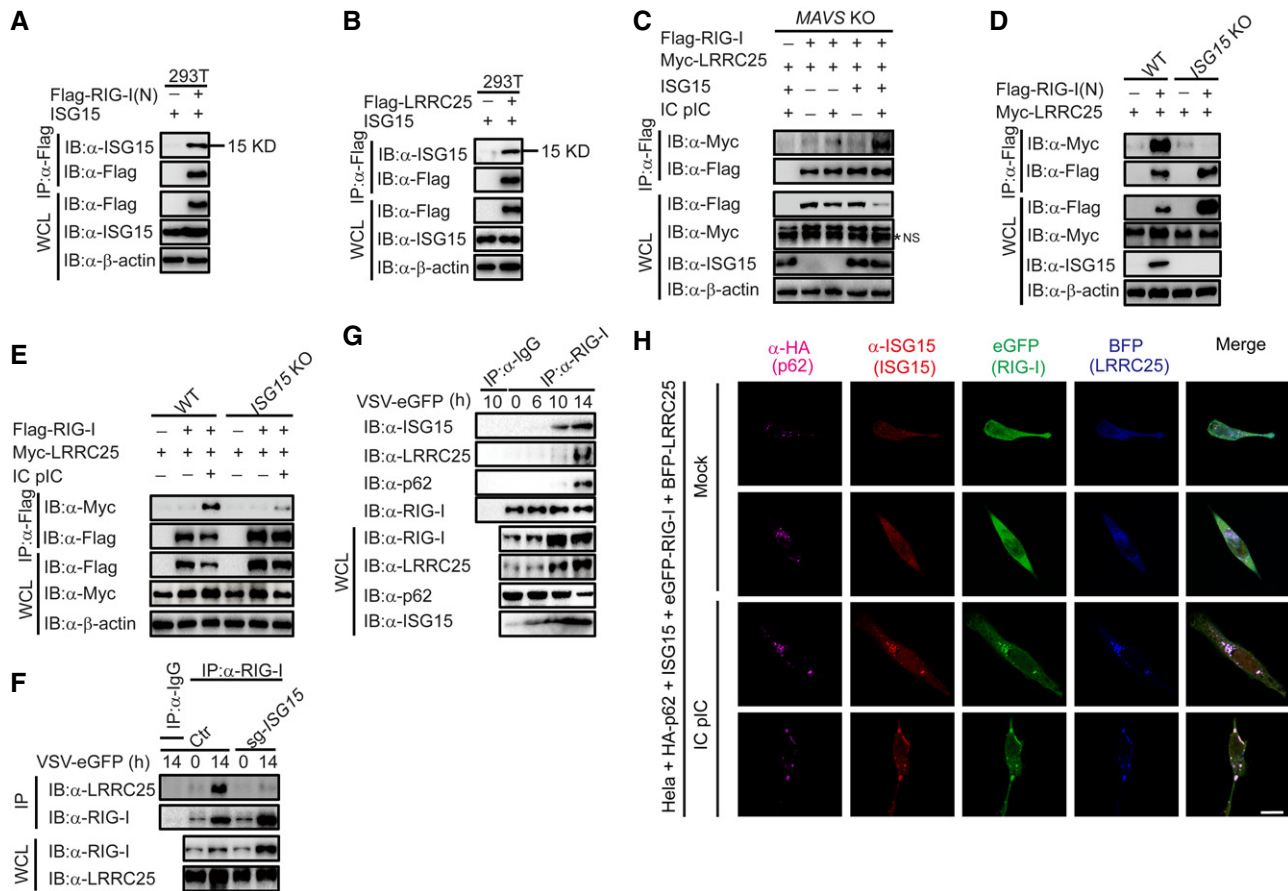A, B   HEK293T cells were transfected with *ISG15*, together with *Flag-RIG-I (N)* (A) or *Flag-LRRC25* (B). 24 h post-transfection, cell lysates were immunoprecipitated using anti-Flag, followed by immunoblot using the indicated antibodies.

C   *MAVS* KO HEK293T cells were transfected with *Flag-RIG-I* and *Myc-LRRC25*, together with an empty vector or *ISG15*. After 12 h, the cells were left untreated or treated with IC poly(I:C) (5 µg/ml) for 24 h. Cell lysates were immunoprecipitated using anti-Flag, followed by immunoblots using the indicated antibodies. NS indicates non-specific bands.

D   WT and *ISG15* KO COS7 cells were transfected with *Flag-RIG-I (N)* and *Myc-LRRC25*. 24 h post-transfection, cell lysates were immunoprecipitated using anti-Flag, followed by immunoblot using the indicated antibodies.

E   WT and *ISG15* KO COS7 cells were transfected with *Flag-RIG-I* and *Myc-LRRC25*. After 12 h, the cells were left untreated or treated with IC poly(I:C) (5 µg/ml) for 24 h. Cell lysates were immunoprecipitated using anti-Flag, followed by immunoblots using the indicated antibodies.

F   Control and *ISG15* KO THP-1 cells were infected with VSV-eGFP (MOI = 0.1) for 14 h. Cell lysates were immunoprecipitated using anti-RIG-I, followed by immunoblots using anti-LRRC25.

G   THP-1 cells were infected with VSV-eGFP (MOI = 0.2) for indicated time points, and cell lysates were immunoprecipitated using anti-RIG-I, followed by immunoblots using indicated antibodies.

H   Confocal microscopic analysis of HeLa cells co-transfected with *HA-p62*, *ISG15*, *eGFP-RIG-I*, and *BFP-LRRC25*, followed IC poly(I:C) (5 µg/ml) treatment for 24 h. Scale bar, 20 µm.

Data information: In (A–H), data are representative of three independent experiments.

negatively regulates RIG-I level (Kim *et al*, 2008). However, its molecular mechanism is yet to be understood. We reasoned that ISG15 might contribute to the degradation of RIG-I mediated by LRRC25. As expected, we observed that LRRC25 could destabilize RIG-I (N) in the presence of ISG15 in *MAVS* KO HEK293T cells (Fig 6G). To further confirm these findings, we constructed *ISG15* KO COS7 cells and THP-1 cells using the CRISPR/Cas9 system (Fig EV5A and B). We found that the degradation of RIG-I (N) and endogenous RIG-I mediated by LRRC25 was abrogated in the absence of ISG15 (Fig 6H and I). In addition, we observed that endogenous RIG-I was markedly reduced after treatment of

cycloheximide (CHX), when ISG15 was ectopically expressed in control cells compared to that in LRRC25 knockout cells (Fig EV5C). These results suggest that LRRC25 degrades RIG-I in an ISG15-dependent manner.

The interaction between RIG-I and LRRC25 is dependent on ISG15

Although previous reports showed that RIG-I undergoes ISGyla-tion upon viral infection (Kim *et al*, 2008), we observed that both RIG-I (N) and LRRC25 could interact with ISG15 in an unconju-gated manner in HEK293T cells (Fig 7A and B). Consistently,
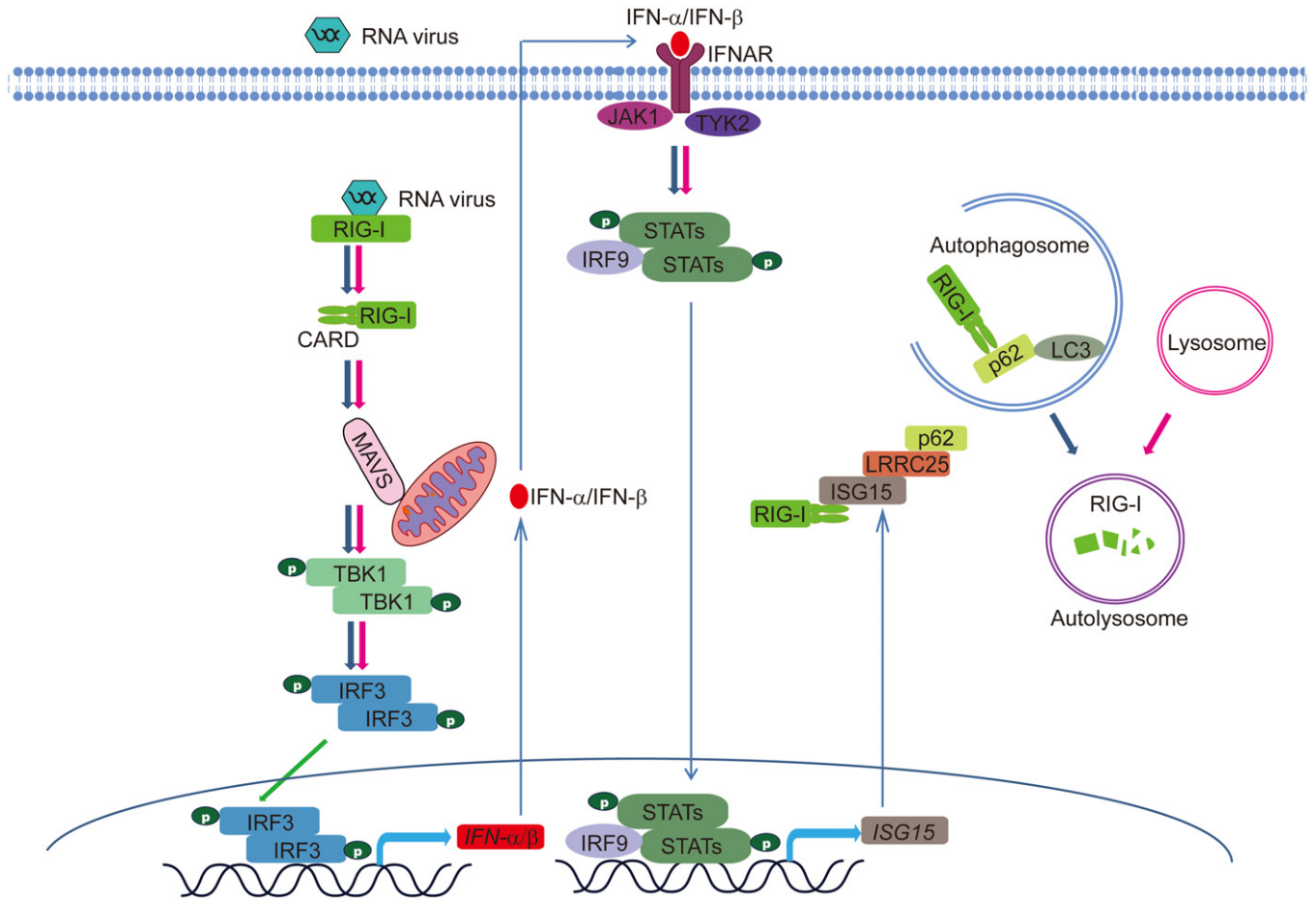
Figure 8. A proposed working model to illustrate how the ISG15-LRRC25-p62 axis negatively regulates type I IFN signaling.

conjugation-defect mutation (LRLRAA) of ISG15 still interacted with RIG-I (N) (Fig EV5D) and with LRRC25 (Fig EV5E). Both wild-type ISG15 and mutant ISG15 (LRLRAA) could mediate the degradation of RIG-I (N) by LRRC25 in *MAVS* KO cells (Fig EV5F), suggesting that non-covalent ISG15 promotes the degradation of RIG-I mediated by LRRC25.

Based on these data, we hypothesized that the unconjugated interaction between ISG15 and RIG-I as well as LRRC25 might affect the interaction between RIG-I and LRRC25. As expected, co-IP results showed that the impaired interaction between RIG-I and LRRC25 in *MAVS* KO cells could be restored in the presence of ISG15 after IC poly(I:C) treatment (Fig 7C). However, the interactions between LRRC25 and RIG-I or its CARDs domain were severely impaired in *ISG15* KO cells (Fig 7D and E). Furthermore, the endogenous interaction between RIG-I and LRRC25 was markedly inhibited in *ISG15* KO THP-1 cells after VSV infection (Fig 7F). Notably, the interaction between RIG-I (N) and p62 was completely abolished in the absence of ISG15 (Fig EV5G). However, the deficiency of ISG15 had no effects on the association between LRRC25 and p62 (Fig EV5H). To further confirm the acting sequence of ISG15 after viral infection, we performed immunoprecipitation experiments to evaluate the endogenous interaction between RIG-I, ISG15, LRRC25, and p62 at different time points during the viral infection. Consistent

with our previous data, the immunoprecipitation results showed that after viral infection, RIG-I firstly interacted with ISG15, and then, the ISG15-associated RIG-I interacted with LRRC25 and p62 (Fig 7G). In addition, confocal microscopy also showed that RIG-I, ISG15, LRRC25, and p62 formed puncta upon IC poly(I:C) stimulation (Fig 7H). Taken together, these findings provide strong evidence that ISG15 plays a critical role in the RIG-I-LRRC25 interaction and subsequent autophagic degradation of RIG-I through p62.

Discussion

In this study, we have shown that LRRC25 inhibits RIG-I-mediated type I IFN signaling through a p62-dependent autophagy pathway. LRRC25 functions as a bridge for the interaction between RIG-I and p62. Furthermore, we show that IFN-inducible free ISG15 is required for LRRC25 to interact with RIG-I. Our findings provide a previously unrecognized mechanism by which LRRC25 mediates inhibition of type I IFN signaling by targeting RIG-I for degradation via a selective autophagy pathway. Because RLR-mediated type I IFN signaling plays predominant roles in antiviral immunity, it is critically important to tightly control the activity of RIG-I for avoiding excessive harmful immune response. Several studies have

reported that the activity and stability of RIG-I are regulated by multiple protein modifications. Proteasomal degradation of RIG-I could be initiated through K48-linked ubiquitination by several E3 ligases, including RNF125, CHIP, and Siglec-G/c-Cbl (Arimoto *et al*, 2007; Chen *et al*, 2013; Zhao *et al*, 2016). In addition, the phosphorylation and deamidation also play important roles in the regulation of RIG-I activity. For instance, CKII and PKCα/β negatively regulate the activation of RIG-I through phosphorylating the CTD and CARDs domain of RIG-I, respectively, while PFAS could positively regulate RIG-I via deamidation (Sun *et al*, 2011; Maharaj *et al*, 2012; He *et al*, 2015). Other and our own studies also show that several NLRs, including NLRC5 and NLRX1, could inhibit type I IFN signaling through physically blocking the interaction between RIG-I and MAVS (Cui *et al*, 2010; Allen *et al*, 2011; Xia *et al*, 2011). However, whether RIG-I stability is regulated by selective autophagy is not well investigated so far.

Autophagy is an evolutionarily conserved degradation pathway with diverse biological functions in immune response, including intracellular pathogen sensing, antigen presentation, lymphocyte development, and T-cell selection (Starr *et al*, 2003; Dengjel *et al*, 2005; Lee *et al*, 2007; Shin *et al*, 2010; Arsov *et al*, 2011). Many autophagic proteins are involved in the regulation of type I IFN signaling. ATG5-ATG12 has been reported to interfere the interaction between RIG-I and MAVS to down-regulate type I IFN signaling (Jounai *et al*, 2007). Beclin-1 associates with cGAS and restricts cGAS enzymatic activity and subsequently attenuates cGAS-induced antiviral immune response (Liang *et al*, 2014). More recently, we found that Beclin-1 can also inhibit RLR-mediated type I IFN signaling by blocking the interaction between RIG-I and MAVS (Jin *et al*, 2016). p62 has been shown to recognize the poly-ubiquitinated proteins and recruit them to autophagosome through its UBA domain as a cargo receptor for selective degradation (Pankiv *et al*, 2007). However, we found that p62 ΔUBA (lacking ubiquitin-binding domain) still interacts with RIG-I for autophagy degradation, suggesting that the interaction between RIG-I and p62 is independent on poly-ubiquitin signal. In addition, we showed that RIG-I-N (8KR), the RIG-I mutant lacking all the known ubiquitination sites, could still be degraded by LRRC25 through the autophagy pathway. Further experiments show that LRRC25 acts as a secondary receptor to promote p62-mediated autophagic degradation of RIG-I in an ubiquitin signal-independent manner.

To understand the molecular mechanisms by which LRRC25 promotes p62-mediated autophagic degradation of RIG-I, we show that ISG15 is critically required for the p62-mediated degradation of RIG-I. ISG15, an ubiquitin-like protein, is highly induced by type I IFN signaling and exhibits antiviral activities (Skaug & Chen, 2010; Morales & Lenschow, 2013). Increasing evidence indicates that ISG15 mainly exerts its function by either conjugating to the lysine of its targeted proteins or free form (unconjugated ISG15) to regulate type I IFN signaling (Zhao *et al*, 2005; Tang *et al*, 2010; Morales & Lenschow, 2013). However, the functions of ISG15 in mice and humans are different. In ISG15 KO mice, antiviral immune response is reduced or mildly affected (Lenschow *et al*, 2007; Morales & Lenschow, 2013), but ISG15 deficiency in human increases viral resistance and type I IFN production (Zhang *et al*, 2015; Speer *et al*, 2016). It appears that human ISG15 functions as a key negative regulator to inhibit type I IFN signaling and IFN-α/β production via USP18 stabilization (Zhang *et al*, 2015). Although ISG15 has been

suggested to negatively regulate RIG-I-mediated antiviral signaling in a conjugated ISGylation-dependent manner (Kim *et al*, 2008), its precise mechanisms, particularly free ISG15-mediated mechanisms, are still not clear. Recent studies demonstrate that free ISG15 might play a role in antiviral responses. Free ISG15 has been reported to prevent the proteasome-dependent degradation of USP18 to block JAK STAT signaling pathway (Zhang *et al*, 2015; Speer *et al*, 2016; Hermann & Bogunovic, 2017). However, the function of free ISG15 in autophagic degradation has not been reported. Our results presented in this study provide evidence that free ISG15 interacts with RIG-I and acts as an essential recognition signal for LRRC25/p62-mediated autophagic degradation of RIG-I to dampen RIG-I-mediated signaling. We show that LRRC25 deficiency blocks RIG-I degradation after viral infection; similarly, ISG15 KO impairs the interaction of LRRC25 with RIG-I, thus reducing RIG-I degradation. These results suggest that LRRC25 recognizes RIG-I through free ISG15 after activation of RIG-I signaling and targets it for degradation through p62-mediated autophagy pathway. Thus, our results provide macular insights into the regulatory mechanisms of type I IFN signaling through the crosstalk with selective autophagy.

Based on these experimental data, we proposed a working model to illustrate how LRRC25 negatively regulates RLR-mediated type I IFN signaling through facilitating the RIG-I-p62 interaction (Fig 8). Upon RNA virus infection, RIG-I triggers the activation of type I IFN signaling and up-regulates a variety of downstream ISGs, including ISG15. ISG15 then interacts with the CARD domains of RIG-I and enhances the interaction between LRRC25 and RIG-I. As a key secondary receptor, LRRC25 next bridges ISG15-associated RIG-I to cargo receptor p62 and assists RIG-I delivery to autophagosomes for degradation. Thus, the RIG-I/ISG15/LRRC25 axis forms a negative feedback loop to maintain the balance of type I IFN activation.

In summary, our results shed new light on the function of ISG15 and LRRC25 in the regulation of RIG-I mediated type I IFN signaling. More importantly, we have provided compelling evidence that innate immune signaling and selective autophagy are fully integrated. Furthermore, considering the pathological role of RIG-I in many diseases, our findings have identified a novel therapeutic target for developing antiviral and cancer therapies.

Materials and Methods

Cell culture and antibodies

HEK293T (human embryonic kidney 293T) and COS7 cells were cultured in DMEM supplemented with 10% (vol/vol) FBS. Human THP-1 cells and PBMCs were grown in RPMI 1640/glutamine medium (Gibco) containing 10% (vol/vol) fetal bovine serum (Gibco). The antibodies used in this study were purchased from indicated companies: Anti-c-Myc-HRP (11814150001) and HRP-anti-hemagglutinin (12013819001) were purchased from Roche Applied Science; anti-β-actin (A1978) and horseradish peroxidase (HRP)-anti-Flag (M2) (A8592) were purchased from Sigma; anti-IRF3 (sc-9082), anti-MAVS (E-3) (sc-166583), and anti-GFP (sc-8334) were purchased from Santa Cruz Biotechnology; anti-RIG-I (#3743), anti-p-IRF3 (#4947S), anti-Beclin-1 (#3738), anti-ATG5 (#12994S), anti-ISG15 (#2743), anti-mouse IgG-HRP (#7076), and anti-rabbit IgG-HRP (#7074) were purchased from Cell Signaling Technology;

anti-LRRC25 (#AB84954) was purchased from Abcam; and anti-p62 (#18420-1-AP) was purchased from proteintech.

Transfection and reporter assays

HEK293T cells were plated in 96-well plates and transfected, using Lipofectamine 2000 (Invitrogen), with plasmids encoding an ISRE or IFN-β luciferase reporter (firefly luciferase; 25 ng) and pRL-TK (renilla luciferase plasmid; 3 ng) together with 25 ng expression vector of Flag-RIG-I (N), Flag-cGAS, Flag-STING, Flag-MAVS, Flag-TBK1, Flag-IRF3, or Flag-MDA5, and increasing concentrations (0, 50, or 100 ng) of plasmid expressing LRRC25 or domain deletions of LRRC25. Empty pcDNA3.1 vector was used to maintain equal amounts of DNA among wells. Cells were collected at 24–36 h after transfection, and luciferase activity was measured with a Dual-Luciferase Assay (Promega) with a Luminoskan Ascent luminometer (Thermo Scientific) according to the manufacturer's protocol. Reporter gene activity was determined by normalization of the firefly luciferase activity to renilla luciferase activity. Because poly(I:C)-low molecular weight (LMW) is a specific ligand for RIG-I but not for MDA5 (Kato *et al*, 2008; Takeuchi & Akira, 2010), we used poly(I:C)-LMW as a RIG-I ligand in this study (Invivogen (Catalog # tlrl-picwlv).

Virus infection

VSV-eGFP and Sendai virus were kindly provided by Dr. Xiaofeng Qin (Sun Yat-sen University). Human influenza virus A/Puerto Rico/8/34 (H1N1) (PR8) was kindly provided by Dr. Hui Zhang (Zhongshan Medical School, Sun Yat-sen University). Cells were infected at various MOI, as previously described by Cui *et al* (2012) and Shapira *et al* (2009).

siRNA transfection

siRNA targeting human LRRC25 was chemically synthesized from TranSheepBio and transfected using Lipofectamine® RNAiMAX (Invitrogen) according to the manufacturer's protocols. Oligonucleotide sequences are as follows:
LRRC25 siRNA #1:
Sense: 5′-GCACCAGUGGGAUGAACAA-3′
Anti-sense: 5′-UUGUUCAUCCCACUGGUGC-3′
LRRC25 siRNA #2:
Sense: 5′-CUCCCGACUAUGAGAACAU-3′
Anti-sense: 5′-AUGUUCUCAUAGUCGGGAG-3′

Real-time PCR

Total RNA was isolated using TRIzol reagent (Invitrogen) and subjected to reverse transcription using PrimeScriptTM RT Master Mix (TAKARA). All gene transcripts were quantified by real-time PCR with SYBR green qPCR Mix kit (Genstar). The following primers were used for real-time PCR:
IFNβ:
Forward 5′-CCTACAAAGAAGCAGCAA-3′
Reverse 5′-TCCTCAGGGATGTCAAAG-3′
IFIT2:
Forward 5′-GGAGGGAGAAAACTCCTTGGA-3′
Reverse 5′-GGCCAGTAGGTTGCACATTGT-3′

IFIT1:
Forward 5′-TCAGGTCAAGGATAGTCTGGAG-3′
Reverse 5′-AGGTTGTGTATTCCCACACTGTA-3′
GAPDH:
Forward 5′-TCAAGAAGGTGGTGAAGCAG-3′
Reverse 5′-GAGGGGAGATTCAGTGTGGT-3′
LRRC25:
Forward 5′-TGCTACGCAACCCCTTGTC-3′
Reverse 5′-GGCCAGAGCAGTTGTCTCG-3′
RIG-I (N):
Forward 5′-CTGCAAGCCTTCCAGGATTATAT-3′
Reverse 5′-TCTGATCTGAGAAGGCATTCCA-3′

ELISA

Control or *LRRC25* KO THP-1 cells were infected with VSV-eGFP (MOI: 0.01) for 36 h. Cell culture supernatants were harvested and analyzed for IFN-β production using a human IFN-β ELISA kit (Cloud-Clone Corp) according to the manufacturer's protocols.

Immunoprecipitation and immunoblot analysis

For immunoprecipitation, whole-cell extracts were prepared after transfection or stimulation with appropriate ligands, followed by incubation overnight with the appropriate antibodies plus protein A/G beads (Pierce) or anti-Flag agarose gels (Sigma) were used. Beads were then washed five times with low-salt lysis buffer, and immunoprecipitates were eluted with 3× SDS loading buffer and resolved by SDS–PAGE. Proteins were transferred to PVDF or NC membranes (Bio-Rad) and further incubated with the appropriate antibodies. Immobilon Western chemiluminescent HRP substrate (Millipore) was used for protein detection.

Generation of *LRRC25* KO cells by the CRISPR/Cas9 technology

LRRC25 KO THP-1 cells were generated by the CRISPR/Cas9 system, and the sequences of target sgRNA are as follows:
LRRC25-sgRNA:
Forward 5′-CACCGTGTCCTCCGCGGATGTGG-3′
Reverse 5′-CCACATCCGCGGAGGACACGGTG-3′

Expanded View for this article is available online.

Author contributions

YD, R-FW, and JC designed the study; YD, TD, YF, QL and ML performed the experiments and analyzed the results. YD, JC, and R-FW prepared the manuscript.

Conflict of interest

The authors declare that they have no conflict of interest.

References

Allen IC, Moore CB, Schneider M, Lei Y, Davis BK, Scull MA, Gris D, Roney KE, Zimmermann AG, Bowzard JB, Ranjan P, Monroe KM, Pickles RJ, Sambhara S, Ting JP (2011) NLRX1 protein attenuates inflammatory responses to infection by interfering with the RIG-I-MAVS and TRAF6-NF-kappaB signaling pathways. *Immunity* 34: 854–865

Arimoto K, Takahashi H, Hishiki T, Konishi H, Fujita T, Shimotohno K (2007) Negative regulation of the RIG-I signaling by the ubiquitin ligase RNF125. *Proc Natl Acad Sci USA* 104: 7500–7505

Arsov I, Adebayo A, Kucerova-Levisohn M, Haye J, MacNeil M, Papavasiliou FN, Yue Z, Ortiz BD (2011) A role for autophagic protein beclin 1 early in lymphocyte development. *J Immunol* 186: 2201–2209

Chen W, Han C, Xie B, Hu X, Yu Q, Shi L, Wang Q, Li D, Wang J, Zheng P, Liu Y, Cao X (2013) Induction of Siglec-G by RNA viruses inhibits the innate immune response by promoting RIG-I degradation. *Cell* 152: 467–478

Cui J, Zhu L, Xia X, Wang HY, Legras X, Hong J, Ji J, Shen P, Zheng S, Chen ZJ, Wang RF (2010) NLRC5 negatively regulates the NF-kappaB and type I interferon signaling pathways. *Cell* 141: 483–496

Cui J, Li Y, Zhu L, Liu D, Songyang Z, Wang HY, Wang RF (2012) NLRP4 negatively regulates type I interferon signaling by targeting the kinase TBK1 for degradation via the ubiquitin ligase DTX4. *Nat Immunol* 13: 387–395

Dengjel J, Schoor O, Fischer R, Reich M, Kraus M, Muller M, Kreymborg K, Altenberend F, Brandenburg J, Kalbacher H, Brock R, Driessen C, Rammensee HG, Stevanovic S (2005) Autophagy promotes MHC class II presentation of peptides from intracellular source proteins. *Proc Natl Acad Sci USA* 102: 7922–7927

He S, Zhao J, Song S, He X, Minassian A, Zhou Y, Zhang J, Brulois K, Wang Y, Cabo J, Zandi E, Liang C, Jung JU, Zhang X, Feng P (2015) Viral pseudo-enzymes activate RIG-I via deamidation to evade cytokine production. *Mol Cell* 58: 134–146

Hermann M, Bogunovic D (2017) ISG15. In sickness and in health. *Trends Immunol* 38: 79–93

Inohara N, Chamaillard M, McDonald C, Nunez G (2005) NOD-LRR proteins: role in host-microbial interactions and inflammatory disease. *Annu Rev Biochem* 74: 355–383

Jin S, Tian S, Chen Y, Zhang C, Xie W, Xia X, Cui J, Wang RF (2016) USP19 modulates autophagy and antiviral immune responses by deubiquitinating Beclin-1. *EMBO J* 35: 866–880

Jounai N, Takeshita F, Kobiyama K, Sawano A, Miyawaki A, Xin KQ, Ishii KJ, Kawai T, Akira S, Suzuki K, Okuda K (2007) The Atg5 Atg12 conjugate associates with innate antiviral immune responses. *Proc Natl Acad Sci USA* 104: 14050–14055

Kato H, Takeuchi O, Mikamo-Satoh E, Hirai R, Kawai T, Matsushita K, Hiiragi A, Dermody TS, Fujita T, Akira S (2008) Length-dependent recognition of double-stranded ribonucleic acids by retinoic acid–inducible gene-I and melanoma differentiation–associated gene 5. *J Exp Med* 205: 1601–1610

Kawai T, Takahashi K, Sato S, Coban C, Kumar H, Kato H, Ishii KJ, Takeuchi O, Akira S (2005) IPS-1, an adaptor triggering RIG-I- and Mda5-mediated type I interferon induction. *Nat Immunol* 6: 981–988

Kim MJ, Hwang SY, Imaizumi T, Yoo JY (2008) Negative feedback regulation of RIG-I-mediated antiviral signaling by interferon-induced ISG15 conjugation. *J Virol* 82: 1474–1483

Kuma A, Matsui M, Mizushima N (2007) LC3, an autophagosome marker, can be incorporated into protein aggregates independent of autophagy: caution in the interpretation of LC3 localization. *Autophagy* 3: 323–328

Lee HK, Lund JM, Ramanathan B, Mizushima N, Iwasaki A (2007) Autophagy-dependent viral recognition by plasmacytoid dendritic cells. *Science* 315: 1398–1401

Lenschow DJ, Lai C, Frias-Staheli N, Giannakopoulos NV, Lutz A, Wolff T, Osiak A, Levine B, Schmidt RE, Garcia-Sastre A, Leib DA, Pekosz A, Knobeloch KP, Horak I, Virgin HW IV (2007) IFN-stimulated gene 15 functions as a critical antiviral molecule against influenza, herpes, and Sindbis viruses. *Proc Natl Acad Sci USA* 104: 1371–1376

Liang Q, Seo GJ, Choi YJ, Kwak MJ, Ge J, Rodgers MA, Shi M, Leslie BJ, Hopfner KP, Ha T, Oh BH, Jung JU (2014) Crosstalk between the cGAS DNA sensor and Beclin-1 autophagy protein shapes innate antimicrobial immune responses. *Cell Host Microbe* 15: 228–238

Lin M, Zhao Z, Yang Z, Meng Q, Tan P, Xie W, Qin Y, Wang RF, Cui J (2016) USP38 inhibits type I interferon signaling by editing TBK1 ubiquitination through NLRP4 signalosome. *Mol Cell* 64: 267–281

Loo YM, Gale M Jr (2011) Immune signaling by RIG-I-like receptors. *Immunity* 34: 680–692

Maharaj NP, Wies E, Stoll A, Gack MU (2012) Conventional protein kinase C-α (PKC-α) and PKC-β negatively regulate RIG-I antiviral signal transduction. *J Virol* 86: 1358–1371

Matsumoto G, Shimogori T, Hattori N, Nukina N (2015) TBK1 controls autophagosomal engulfment of polyubiquitinated mitochondria through p62/SQSTM1 phosphorylation. *Hum Mol Genet* 24: 4429–4442

Meylan E, Curran J, Hofmann K, Moradpour D, Binder M, Bartenschlager R, Tschopp J (2005) Cardif is an adaptor protein in the RIG-I antiviral pathway and is targeted by hepatitis C virus. *Nature* 437: 1167–1172

Morales DJ, Lenschow DJ (2013) The antiviral activities of ISG15. *J Mol Biol* 425: 4995–5008

Ng AC, Eisenberg JM, Heath RJ, Huett A, Robinson CM, Nau GJ, Xavier RJ (2011) Human leucine-rich repeat proteins: a genome-wide bioinformatic categorization and functional analysis in innate immunity. *Proc Natl Acad Sci USA* 108(Suppl 1): 4631–4638

O'Neill LAJ (2006) How Toll-like receptors signal: what we know and what we don't know. *Curr Opin Immunol* 18: 3–9

Pankiv S, Clausen TH, Lamark T, Brech A, Bruun JA, Outzen H, Overvatn A, Bjorkoy G, Johansen T (2007) p62/SQSTM1 binds directly to Atg8/LC3 to facilitate degradation of ubiquitinated protein aggregates by autophagy. *J Biol Chem* 282: 24131–24145

Seth RB, Sun L, Ea CK, Chen ZJ (2005) Identification and characterization of MAVS, a mitochondrial antiviral signaling protein that activates NF-kappaB and IRF 3. *Cell* 122: 669–682

Shapira SD, Gat-Viks I, Shum BO, Dricot A, de Grace MM, Wu L, Gupta PB, Hao T, Silver SJ, Root DE, Hill DE, Regev A, Hacohen N (2009) A physical and regulatory map of host-influenza interactions reveals pathways in H1N1 infection. *Cell* 139: 1255–1267

Shin DM, Jeon BY, Lee HM, Jin HS, Yuk JM, Song CH, Lee SH, Lee ZW, Cho SN, Kim JM, Friedman RL, Jo EK (2010) Mycobacterium tuberculosis eis regulates autophagy, inflammation, and cell death through redox-dependent signaling. *PLoS Pathog* 6: e1001230

Skaug B, Chen ZJ (2010) Emerging role of ISG15 in antiviral immunity. *Cell* 143: 187–190

Speer SD, Li Z, Buta S, Payelle-Brogard B, Qian L, Vigant F, Rubino E, Gardner TJ, Wedeking T, Hermann M, Duehr J, Sanal O, Tezcan I, Mansouri N, Tabarsi P, Mansouri D, Francois-Newton V, Daussy CF, Rodriguez MR, Lenschow DJ *et al* (2016) ISG15 deficiency and increased viral resistance in humans but not mice. *Nat Commun* 7: 11496

Starr TK, Jameson SC, Hogquist KA (2003) Positive and negative selection of T cells. *Annu Rev Immunol* 21: 139−176

Stolz A, Ernst A, Dikic I (2014) Cargo recognition and trafficking in selective autophagy. *Nat Cell Biol* 16: 495−501

Sun Z, Ren H, Liu Y, Teeling JL, Gu J (2011) Phosphorylation of RIG-I by casein kinase II inhibits its antiviral response. *J Virol* 85: 1036−1047

Sun L, Wu J, Du F, Chen X, Chen ZJ (2013) Cyclic GMP-AMP synthase is a cytosolic DNA sensor that activates the type I interferon pathway. *Science* 339: 786−791

Takaoka A, Wang Z, Choi MK, Yanai H, Negishi H, Ban T, Lu Y, Miyagishi M, Kodama T, Honda K, Ohba Y, Taniguchi T (2007) DAI (DLM-1/ZBP1) is a cytosolic DNA sensor and an activator of innate immune response. *Nature* 448: 501−505

Takeuchi O, Akira S (2010) Pattern recognition receptors and inflammation. *Cell* 140: 805−820

Tang Y, Zhong G, Zhu L, Liu X, Shan Y, Feng H, Bu Z, Chen H, Wang C (2010) Herc5 attenuates influenza A virus by catalyzing ISGylation of viral NS1 protein. *J Immunol* 184: 5777−5790

Unterholzner L, Keating SE, Baran M, Horan KA, Jensen SB, Sharma S, Sirois CM, Jin T, Latz E, Xiao TS, Fitzgerald KA, Paludan SR, Bowie AG (2010) IFI16 is an innate immune sensor for intracellular DNA. *Nat Immunol* 11: 997−1004

Xia X, Cui J, Wang HY, Zhu L, Matsueda S, Wang Q, Yang X, Hong J, Songyang Z, Chen Z, Wang R-F (2011) NLRX1 negatively regulates TLR-induced NF-κB signaling by targeting TRAF6 and IKK. *Immunity* 34: 843−853

Xu LG, Wang YY, Han KJ, Li LY, Zhai Z, Shu HB (2005) VISA is an adapter protein required for virus-triggered IFN-beta signaling. *Mol Cell* 19: 727−740

Zhang Z, Yuan B, Bao M, Lu N, Kim T, Liu YJ (2011) The helicase DDX41 senses intracellular DNA mediated by the adaptor STING in dendritic cells. *Nat Immunol* 12: 959−965

Zhang X, Bogunovic D, Payelle-Brogard B, Francois-Newton V, Speer SD, Yuan C, Volpi S, Li Z, Sanal O, Mansouri D, Tezcan I, Rice GI, Chen C, Mansouri N, Mahdaviani SA, Itan Y, Boisson B, Okada S, Zeng L, Wang X *et al* (2015) Human intracellular ISG15 prevents interferon-alpha/beta over-amplification and auto-inflammation. *Nature* 517: 89−93

Zhao C, Denison C, Huibregtse JM, Gygi S, Krug RM (2005) Human ISG15 conjugation targets both IFN-induced and constitutively expressed proteins functioning in diverse cellular pathways. *Proc Natl Acad Sci USA* 102: 10200−10205

Zhao K, Zhang Q, Li X, Zhao D, Liu Y, Shen Q, Yang M, Wang C, Li N, Cao X (2016) Cytoplasmic STAT4 promotes antiviral type I IFN production by blocking CHIP-mediated degradation of RIG-I. *J Immunol* 196: 1209−1217